

Study of the radiation hardness of CsI(Tl) scintillation crystals

D.M.Beylin, A.I.Korchagin, A.S.Kuzmin,
L.M.Kurdadze, S.B.Oreshkin, S.E.Petrov, B.A.Shwartz *

*Budker Institute of Nuclear Physics
630090 Novosibirsk, Russia*

Abstract

This paper is devoted to the study of a degradation of CsI(Tl) crystals scintillation characteristics under irradiation with γ -quanta at the uniformly distributed absorbed dose up to 3700 rad. The sample set consisted of 25 crystals of 30 cm long having a truncated pyramid shape and 30 rectangular crystals of the same length. A large difference in the light output deterioration caused by the radiation was observed for the samples of the same shape. A substantial dependence of the average light output loss from the sample shape is seen as well. On the other hand, the crystals from the same ingot behave very similarly under irradiation.

PACS: 29.40.Vj, 29.40.Mc

Keywords: Scintillators, crystals, radiation hardness

* contact author, e-mail: shwartz@inp.nsk.su

1 Introduction

Scintillating crystals of cesium iodide are widely used in high energy physics for photon detection. Calorimeters made of CsI crystals achieve the best energy resolution for photons and electrons [1, 2].

One of the important characteristics of scintillating materials is their radiation hardness, i.e. their ability to retain scintillation efficiency and uniformity over the crystal volume after exposure to ionizing radiation. The radiation hardness of CsI crystals has been previously studied in [3, 4, 5, 6]. Each of these studies was performed with a set of few crystals of different sizes and shapes, produced by different manufacturers. Despite the large spread of the results, it could be deduced that the CsI crystals keep the scintillating properties at the acceptable level after the absorption of a radiation dose up to a few hundred rads. Also, it was clear, that the degradation of scintillating properties of crystals depends significantly on growing technology, raw material quality and size of the crystals.

The interest to the radiation hardness of this material increased with the development and construction of B-, ϕ -, $c - \tau$ factories, e.g storage rings with high luminosity which implies high electron and positron currents, causing high radiation dose absorbed by the detector components. Recently, this subject became topical again due to the development of new B-factory projects with super high luminosity [7, 8].

This study was motivated by an active participation of BINP in the development and construction of the electromagnetic calorimeter of the BELLE detector [9], in operation now at the KEKB collider with luminosity of $10^{34} \text{ cm}^{-2}\text{s}^{-1}$. The electromagnetic calorimeter of this detector contains 8736 crystals of CsI (Tl). Crystals are truncated pyramids of 300 mm length and transverse dimensions of 50-60mm. About 2/3 of the calorimeter elements were produced by BINP in collaboration with the Institute for Single Crystals of National Academy of Sciences of Ukraine (Kharkov). To achieve and retain high energy and spatial resolution of the calorimeter it is important that the light output and uniformity of the crystals do not change significantly over a few years of the experiments at the collider. Therefore, crystals had to pass rather high requirements on radiation hardness.

During initial stages of the calorimeter development, the studies of the radiation hardness of crystals were performed with a few samples [10, 5]. These studies demonstrated that crystals satisfy the requirements.

This paper is devoted to study the radiation hardness of CsI(Tl) crystals using a large number of full size samples. All 55 studied crystals were grown using the same technology by Joint Enterprise "Amcrys-H" of Scientific and

Technological Concern "Institute for Single Crystals", Kharkov, Ukraine. Raw material for all crystals, high purity CsI, was supplied by Novosibirsk Plant of Rare Metals. For irradiation of the samples we used wide bremsstrahlung γ -quanta beam, produced by the 1.4 MeV electron accelerator, ELV-6, at BINP SB RAS. The absorbed dose was distributed nearly uniformly over the crystal volume. Another feature of this work is that the absorbed radiation dose were measured with the detector based on CsI(Tl), thus avoiding error-prone recalculation of this value depending on the radiation energy spectrum. Preliminary results were reported at the INSTR-99 conference [12].

2 Studied samples and measurements of their scintillation properties

From 55 studied samples, 25 were selected from crystals produced for the electromagnetic calorimeter of the BELLE detector. These crystals failed stringent geometry specifications or had small mechanical defects but their scintillation properties met requirements. The samples, further referred as type "B", have a shape of truncated pyramid of 300 mm height and average transverse sizes of about $60 \times 60 \text{ mm}^2$. Detailed description of crystals used in the Belle detector is given in [11]. The studied set comprised the crystals of 16 types which slightly vary in shape and sizes. Area of the large face of the truncated pyramid varies from 35 to 47 cm^2 while the angle between the pyramid sides and the axis ranged from 0.8° to 1.25° , depending on the crystal type.

Other 30 studied samples were shaped as rectangular parallelepiped with sizes of $2 \times 2 \times 30 \text{ cm}^3$. These crystals were specially manufactured for the systematic control of the radiation hardness of the calorimeter elements. These crystals are referred to as crystals of type "P".

Prior to measurements all crystals were polished, wrapped in $200 \mu\text{m}$ porous teflon and covered with $20 \mu\text{m}$ thick aluminized mylar film.

The measurements of the light output of the crystals of type "P" can be done with the photo detector attached to any of two edges of the sample. The light output depends on whether the other end is covered with reflector or not. Marking one end of the crystal as **a**, and the another one as **b**, we classify 4 possible options of the measurements of each crystal in the Table 1. In this work most measurements were performed using method 1. This method is implied throughout the text unless otherwise stated. For all measurements the sides of the crystal were covered by teflon and mylar in the same manner as for the samples of type "B".

To measure the scintillation properties of the crystals we used the setup shown

Table 1

Four options of the light output measurements for crystals of type "P"

Method	Light is measured on	Conditions on the Other End
1	End a	End b is covered with 2 layers of Teflon
2	End a	End b is not covered
3	End b	End a is covered with 2 layers of Teflon
4	End b	End a is not covered

on Fig. 1. Studied crystal is placed vertically on the input window of the two inch PM tube (Hamamatsu R1847-07) with the photocathode without optical contact. Collimated ^{137}Cs radioactive source emits 662 keV photons irradiating about 1 cm wide band of the studied crystal. Signal from the PMT was shaped with shaping amplifier, digitized with ADC and transmitted to the computer.

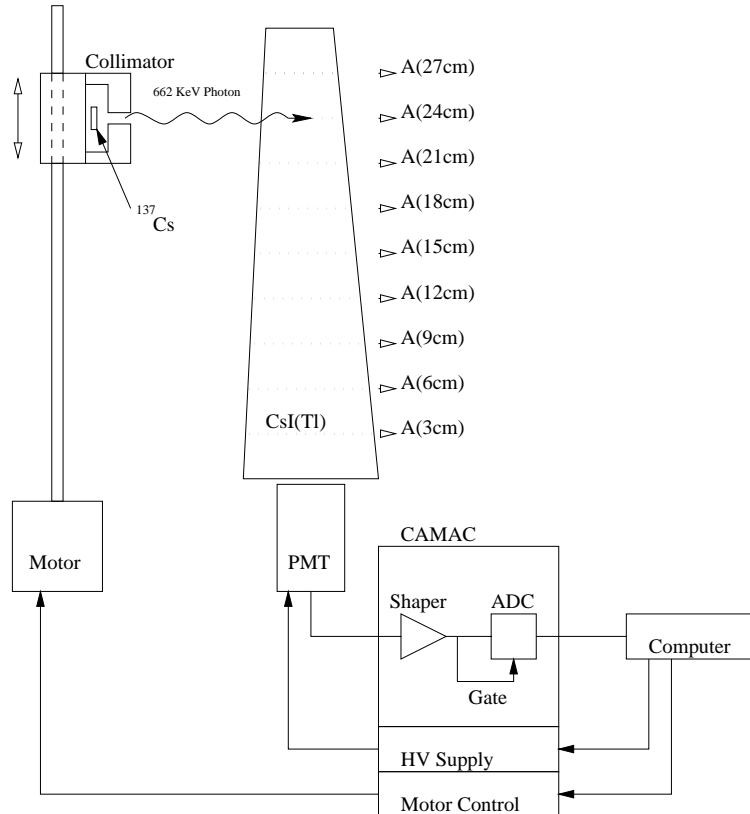


Fig. 1. The light output measurement setup.

Collimator can be moved along the axis of the crystal, irradiating the crystal with γ -quanta at 9 positions every 30 mm. For each source position the pulse height spectrum was measured and the total absorption position was determined. Then the light output was defined as a ratio of this value (A_i) and the

corresponding value for the reference crystal (A_0):

$$L_i = \frac{A_i}{A_0} \times 100\%. \quad (1)$$

Average light output was defined as:

$$\bar{L} = \left(\sum_{i=1}^9 L_i \right) / 9. \quad (2)$$

Non-uniformity of the crystal was defined as:

$$G = \frac{L_{max} - L_{min}}{L} \quad (3)$$

The reference was a CsI(Tl) standard detector of 25mm height and 25mm diameter packed in the aluminum container. Throughout this paper the light output is referred as a ratio to the reference one.

Fig. 2, *a* and *b* represent the distribution of samples of type "B" and "P" over the value of the average light output, measured before the irradiation. It can be seen from the histograms that the initial spread of the light output is rather small.

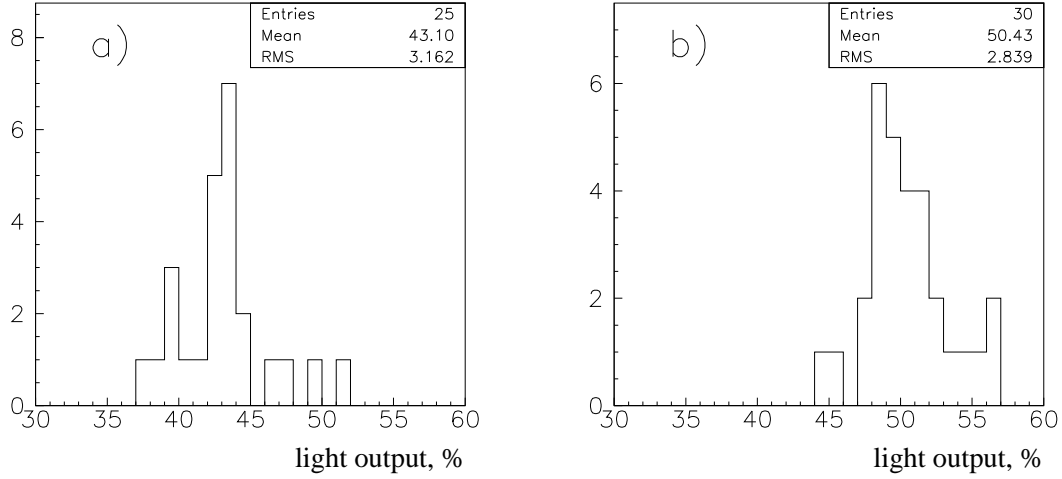


Fig. 2. The light output of the crystals type "B" (*a*) and "P" (*b*) before the irradiation.

3 Irradiation of the Crystals

Accelerator ELV-6 [13] generates continuous 1.4 MeV energy electron beam with up to 100 mA current. The power in the beam reaches 100 kW. The beam with such parameters can produce radiation dose intensity of up to 1

Mrad/hour. This work studied the radiation hardness at moderate doses, and the irradiations were performed at a current that did not exceed 100mA.

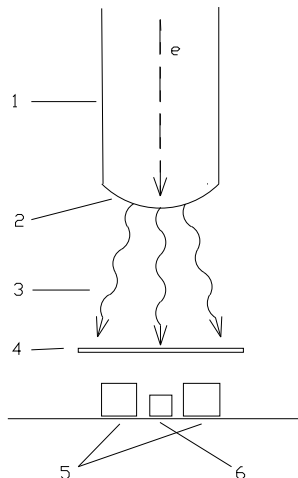


Fig. 3. The setup for irradiation of crystals with the ELV-6 accelerator. 1 – accelerator of electrons ELV-6, 2 – tantalum converter, 3 – bremsstrahlung photons, 4 – 2mm lead plate, 5 – irradiated crystals of CsI(Tl), 6 – detector of radiation dose.

The scheme of the irradiation setup is shown in Fig. 3. The electron beam of 1.4 MeV energy hits the converter (2), composed of 0.5mm Ta, 2mm water and 2mm stainless steel. Bremsstrahlung γ -quanta produced in the converter irradiate crystals (5) located under the beam with its axis perpendicular to the beam direction. Dose detector (6) is placed between the crystals. 2mm plate of lead is used to suppress the low energy part of the photon spectrum.

The resulting photon beam has wide spectra from 0.2 to 1.4 MeV with maximum around 0.6 MeV.

The energy deposited by ionizing radiation in a unit mass of the material is absorbed dose (D). It is measured in units of $1 \text{ Gy} = 1 \text{ J/kg}$. Another unit of absorbed dose is $1 \text{ rad} = 0.01 \text{ Gy}$ ($1 \text{ rad} = 10^{-2} \text{ J/kg} = 5.24 \times 10^8 \text{ MeV/g}$).

The absorbed dose is determined by the radiation intensity and spectra, as well as by the material of the sample. Radiation flux observed by samples consists of the primary radiation and the photons scattered by the surrounding materials. That makes calculation of the absorbed dose difficult even for monochromatic gamma-source. Detectors of absorbed dose are usually based on low- Z materials; this leads to significant systematic errors when re-calculating to CsI. Therefore, for the purpose of this study, we made the dose detector (DD) on the basis of scintillation crystal CsI(Tl). Using the CsI as a detector material we avoid dose recalculation and improve accuracy of absorbed dose measurement.

The layout of the DD is shown in Fig. 4. Scintillation crystal CsI(Tl) with dimensions of $2 \times 2 \times 1 \text{ cm}^3$ is coupled to a vacuum photodiode (PD) with massive photocathode. Photocurrent is proportional to the dose rate in the wide range of the radiation intensity. It is measured by the voltage drop (V) on the load resistor ($R=50\text{K}\Omega$)

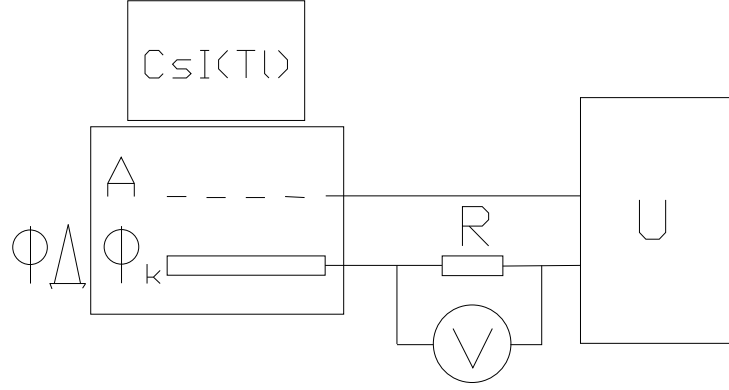


Fig. 4. Detector of absorbed dose. CsI(Tl) - scintillation crystal, PD - Photodiode with massive photocathode, A - Anode, C - photocathode, R - resistor, V - voltmeter, U - DC power supply.

Detailed description of the DD design and calibration procedure is given in Appendix A. It was measured that the intensity of absorbed dose of 1 rad/sec results in a photocurrent of about $0.3 \mu\text{A}$. Then the dose $D(\text{rad})$ absorbed by the crystal during time $t_0(\text{s})$ at the current $I(\mu\text{A})$ can be calculated as:

$$D = \frac{1}{I_R} \int_0^{t_0} I(t) dt,$$

Where $I_R = 0.3 \mu\text{A} \cdot \text{sec/rad}$.

During the irradiation, the current value was recorded every 20 sec. Typical time dependence of the dose rate calculated from the DD current is shown in the Fig. 5.

The relative accuracy of the absorbed dose measurement is about 10% that is determined by the accuracy of DD calibration and taking into account slow scintillation components of CsI(Tl).

Simple estimations show that the multiple scattering of the electrons in the converter result in a good uniformity of the γ -beam over crystal location area. To check this, the transverse profile of the dose intensity at the fixed accelerator current was measured. Nonuniformity was found to be less than 5% within the range from -15cm to 15 cm from the electron beam axis.

The γ -beam used for irradiation has wide energy spectrum from 0.2 to 1.4 MeV

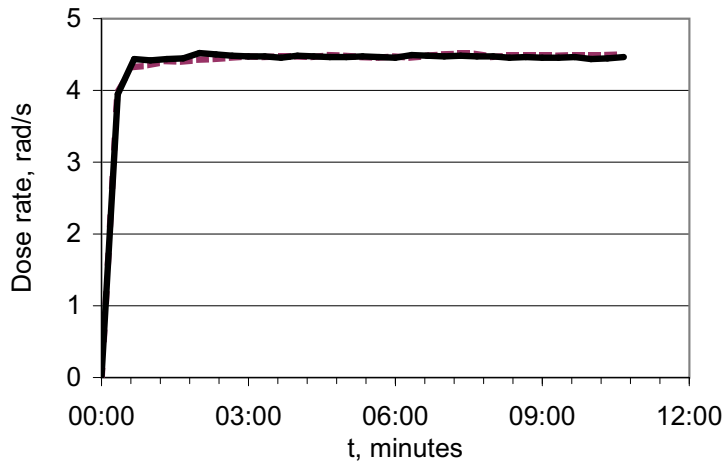


Fig. 5. Typical dose rate in dependence of the time of exposition. Solid line corresponds to the irradiation of crystals from one side, dot line - from the other one (see text).

with maximum around 0.6MeV. At this energy, the average photon interaction length in CsI is about 3 cm. Since the transverse size of the crystal is about 6cm the dose absorbed near the upper side of the crystal is a few times higher than that at the bottom one.

To determine the magnitude of this effect, we performed the following measurement. With certain accelerator current we measured the intensity of the dose absorbed by the DD (J1). Then the DD was shielded with a 6cm thick block of CsI and the measurement was repeated at the same accelerator current (yielding J2). The ratio $k=J1/J2$ was found to be equal to 3.2 which, assuming the exponential dependence of the absorbed dose on the depth, corresponds to the average γ -quanta attenuation length of 5.2cm.

To compensate this nonuniformity each sample was irradiated with equal doses from opposite sides. Fig. 6 shows the dependence of the dose on the depth calculated for $k=3.2$. It can be seen from the picture that nonuniformity of the absorbed dose over the depth is about 15%.

4 Changes of the crystal scintillation characteristics induced by the radiation

The light output of every crystal was measured several times before and after each irradiation. Irradiation sessions were carried out consecutively with 2-6 weeks intervals between them. No more than 3 samples of type "B" or 5 samples of type "P" were irradiated simultaneously in the same session.

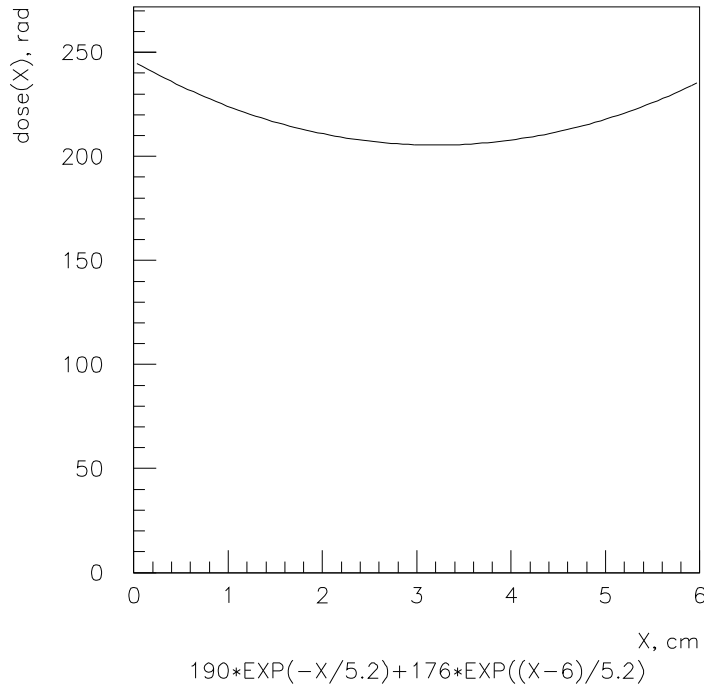


Fig. 6. The distribution of the absorbed dose over the crystal depth after irradiation from both sides.

Significant afterglow of CsI(Tl) makes it difficult to measure the light output right after the irradiation. So, the first measurement was performed only one day after the irradiation when the afterglow became low enough not to broaden and shift the photo-peak significantly.

Fig. 7 shows the average light output of two "P"-type crystals as a function of time. Stability of the measurements performed between the irradiations is better than 1% which allows seeing sharp drops in the light output after irradiations with doses 700 and 3200 rad. Gradual increase in the light output after the second irradiation could be interpreted as a partial recovery of the light-output. This issue will be discussed in more details in the section 6.

4.1 Measurements with the type "B" crystals (pyramids)

From the set of 25 samples shaped as truncated pyramids nine crystals were irradiated several times up to the integrated dose of 3600-3700 rad, six crystals up to 1300-1400 rad, while other 10 samples were irradiated twice — up to 740-780 rad and 3000-3200 rad.

Fig. 8 shows the degradation of the light output, $\Delta L/L$, as a function of the absorbed dose for seven pyramid-shaped crystals (type "B"). As it's seen in the

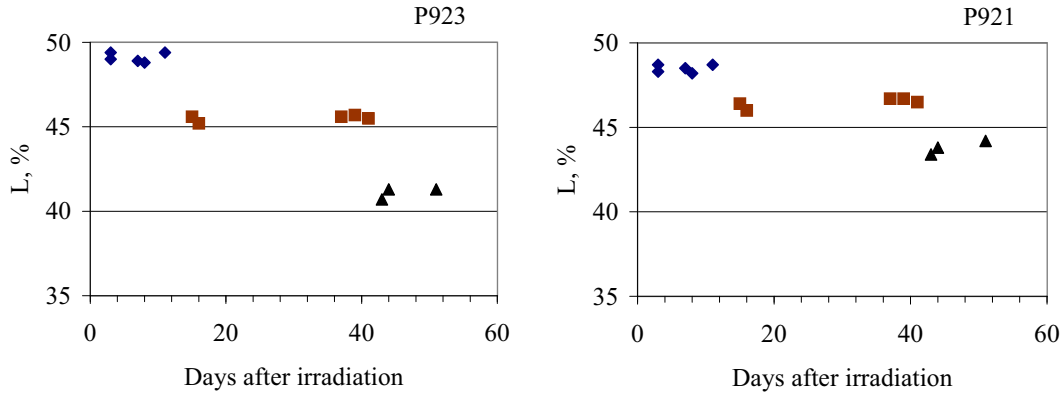


Fig. 7. Light output of two crystals of type "P" as a function of time. \blacklozenge - light-output of the samples before the irradiation, \blacktriangle - after irradiation dose of 700 rad, \blacksquare - after 3200 rad.

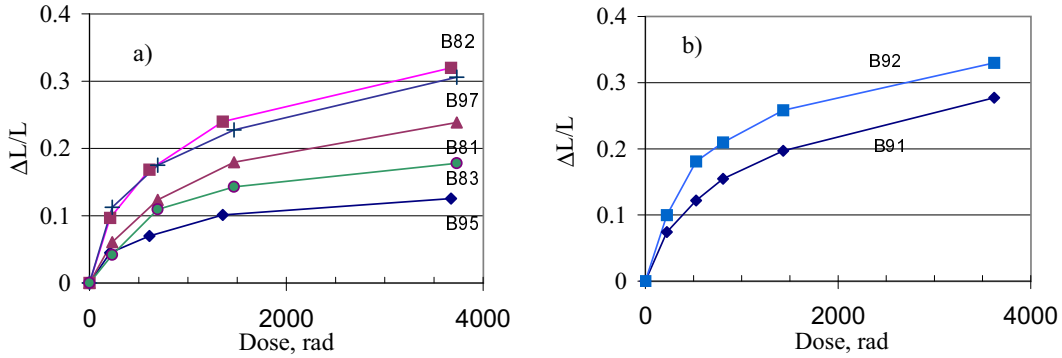


Fig. 8. Light output degradation, $\Delta L/L$, in dependence of the absorbed dose for seven crystals of "B" type.

figure, all crystals are characterized by similar curves. The light output drops fast at the small irradiation doses but at higher doses it decreases slower. For example, for the crystal B91 the drop was 7% after irradiation with 220rad, but only 27% after increase of the dose up to 3.6 Krad.

Fig. 9 shows the distribution of type "B" samples over the light-output loss, $\Delta L/L$, after all irradiations. It can be seen that the distribution is very wide. Thus, after irradiation with 700-800 rad, $\Delta L/L$ varies from 5% to 21%.

As it was mentioned earlier one source of raw material and one technology were used for the production of all studied crystals. Therefore, the wide spread in $\Delta L/L$ is an evidence that the radiation hardness is, probably, strongly dependent on uncontrolled impurities in the raw material or slight variations in the crystal growth regime causing defects in the crystal lattice.

Production of crystals for the electromagnetic calorimeter of the Belle detector, from which the samples studied in this work were selected, took about four years. It took over three years to produce crystals for the barrel part of

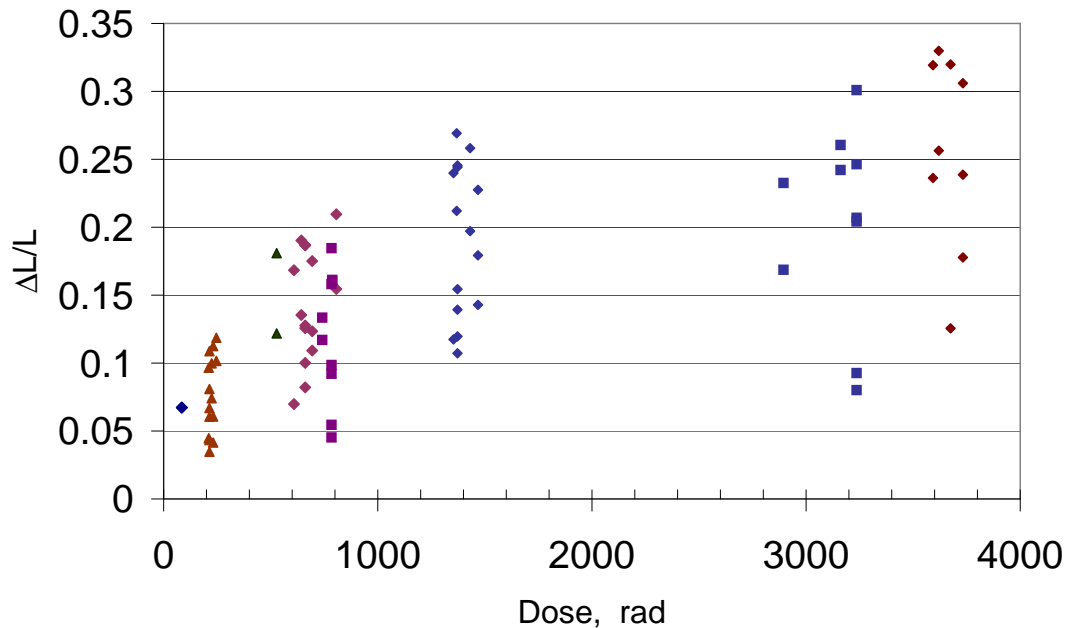


Fig. 9. The light output decrease for all type "B" crystals after all irradiations. Samples of the "endcap" types are marked with \square .

the calorimeter while all the crystals for the endcaps were produced in the last 8 months. One could suppose that over the long production period both growth technology and raw material could vary. In Fig. 9 the endcap type crystals produced near the end of the production are specially marked. As we can see from the picture the distributions over the $\Delta L/L$ for these crystals are very similar to those for the barrel ones.

Fig.10 shows the average values of $\Delta L/L$ as a function of absorbed dose. Points corresponding to the "endcap" crystals are somewhat lower than the rest although the difference is insignificant when compared to the statistical errors.

Values of $\Delta L/L$ obtained in this study do not contradict to the results of the earlier measurements of the radiation hardness of a few samples for the electromagnetic calorimeter of BELLE produced by Crysmatec, Shanghai Institute of Ceramics (SIC) and Kharkov Institute for Single Crystals [5].

We estimate the accuracy of the light output measurements in this work by about 1%. Therefore, the width of the distribution over $\Delta L/L$ at a given absorbed dose (see Fig. 9) is not determined by the measurement errors. This conclusion is supported by a good correlation between the decreases of the light output of the same crystal after irradiation with different doses. Such correlation is presented in Fig.11.

Strong positive correlation which can be seen in Fig. 11 supports the conclusion made earlier that the $\Delta L/L$ dependence on the absorbed dose has similar

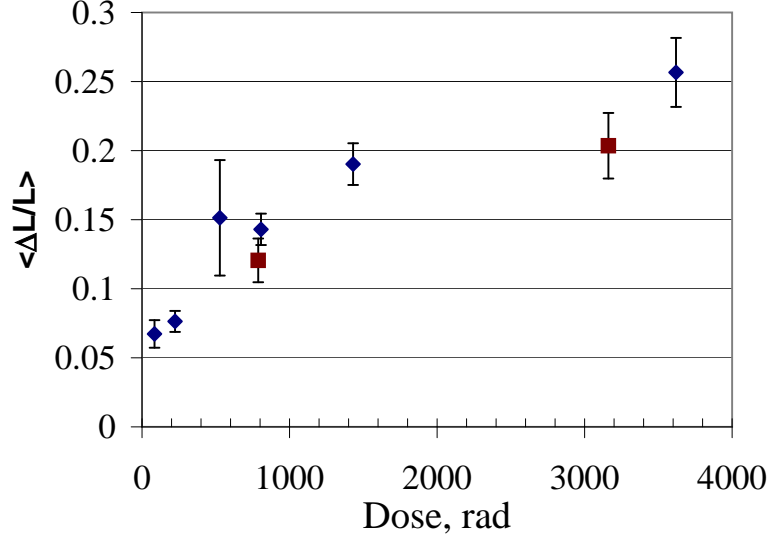


Fig. 10. Average light output deterioration, $\Delta L/L$, for the type "B" crystals as a function of the absorbed dose. The "endcap" samples are marked with \square .

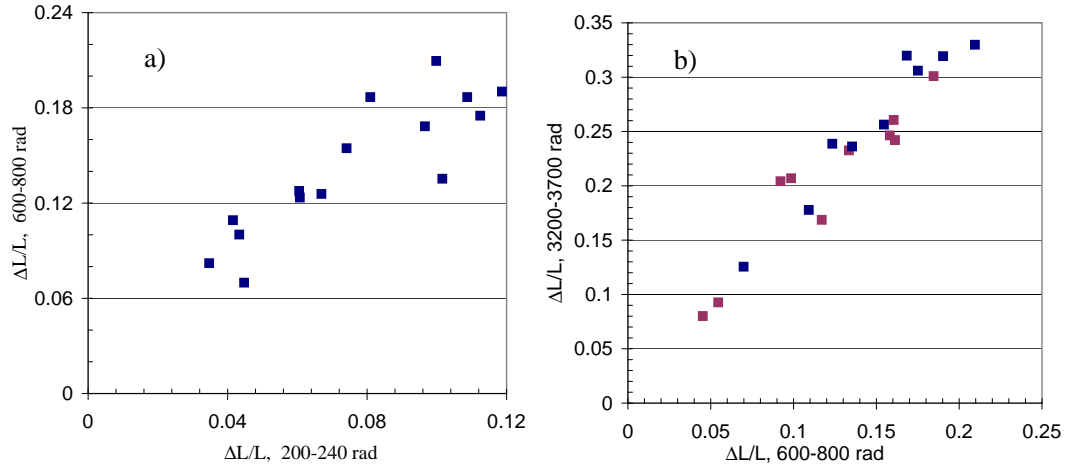


Fig. 11. Correlation between the $\Delta L/L$ for "B" crystals after the irradiation with integrated dose reaches 200÷240 and 600÷800 rad (a), 600÷800 and 3200÷3700 rad (b).

shape for all crystals.

The observed correlation makes possible the procedure of the radiation hardness control for each crystal individually. By measuring the decrease of the light output after irradiation with a relatively small dose and further extrapolating to higher doses, one could come to an expectation about the ability of the crystal to withstand required radiation load.

Another conclusion can be made from the obtained results that if the crystals are to work under high radiation background when radiation hardness is important, it is necessary to study the radiation hardness of sufficiently large set of crystals.

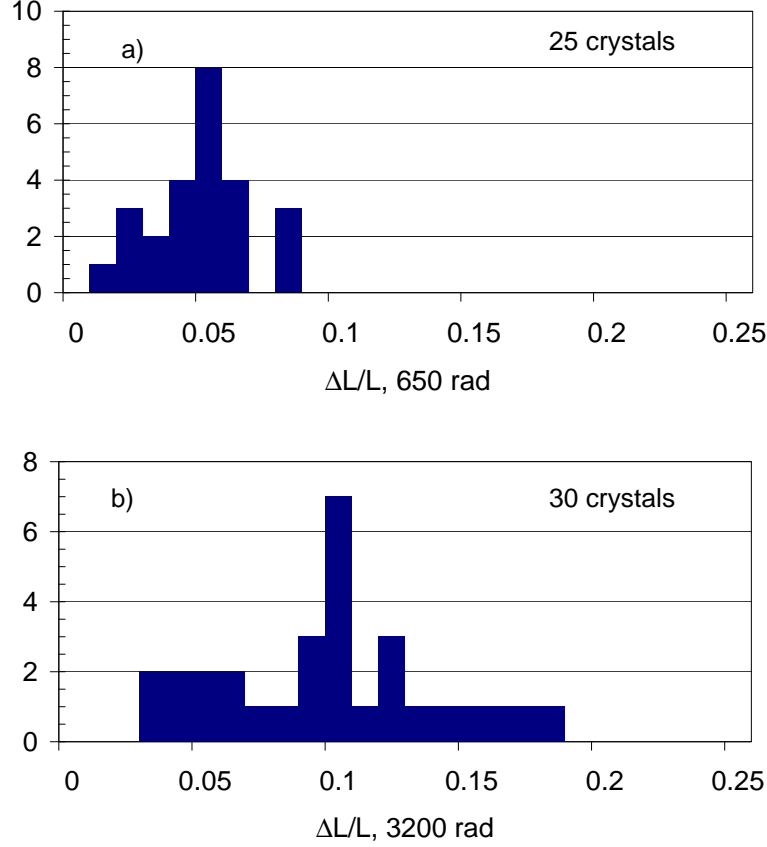


Fig. 12. The distributions of "P" samples over light output deterioration after the irradiation with 650 rad (a) and 3200 rad (b).

Since this work was initiated by the Belle detector construction it should be noted that all the studied samples satisfied the radiation hardness specifications required for the elements of the calorimeter.

It should be noted as well, that some of the studied samples demonstrated very high for the alkali halide crystals radiation hardness ($\Delta L/L=8\%$ at 3.2 Krad). It indicates that the production of the radiation hard CsI crystals is possible after improvements of the growing technology.

4.2 Measurements with the type "P" crystals (parallelepiped)

The set of "P" crystals contained 30 rectangular samples of $2 \times 2 \times 30$ cm³ size. 25 of them were irradiated with 650 rad dose in one exposition and later with additional dose of 2550 rad that resulted in the integrated dose of 3200 rad. 5 crystals were irradiated only once with the dose of 3200 rad.

The distributions over $\Delta L/L$ for "P" samples after the irradiation with 650 and 3200 rad are shown in Fig. 12.

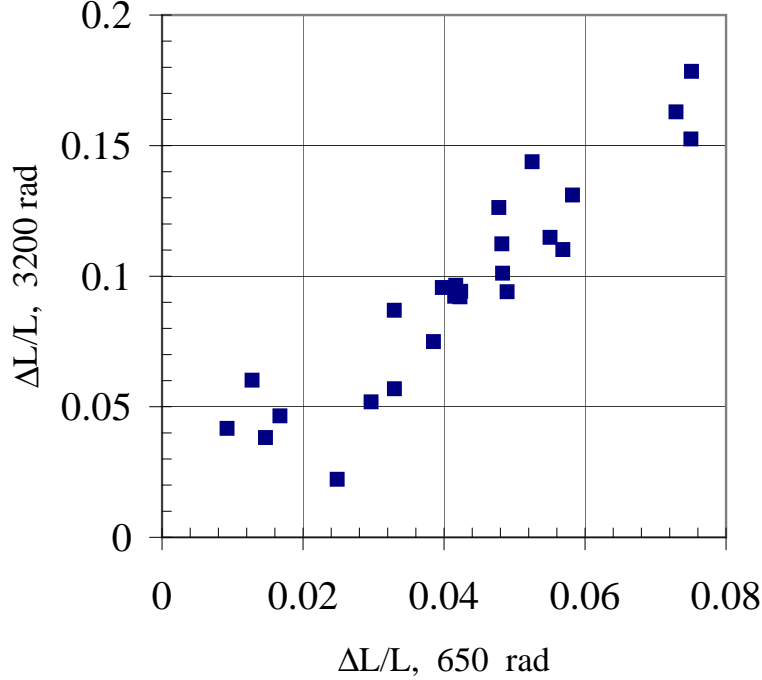


Fig. 13. The correlation between the light output decrease for 25 crystals "P" after the irradiation with 650 rad and 3200 rad.

The distribution is wide like for the "B" crystals case. However, the average decrease is much less — $\langle \Delta L/L \rangle = (4.2 \pm 1.8)\%$ at 650 rad and $\langle \Delta L/L \rangle = (9.0 \pm 3.9)\%$ at 3200 rad. Comparison of these results with those shown in Fig. 10 leads to a conclusion that the light output decrease for parallelepiped shaped crystals is 2-3 times less than that for pyramid ones. This effect will be discussed in more details in the section 8.

The correlation between the light output decrease after the irradiation with 650 rad and 3200 rad is shown in Fig. 13. Similarly to the crystals "B", good correlation between $\Delta L/L$ values after irradiation with various doses is seen.

4.3 The light output change for type "P" crystals at the various light collection conditions

As it was mentioned in the section 2 there are several options for light read out for "P" crystals (see Table 1). To estimate the precision of the $\Delta L/L$ measurement and the influence of the uncontrolled variations in the polishing of the crystal faces as well as wrapping with teflon, we compared the light output after 650 rad dose irradiation measured by option 1 (light is read from the edge **a** while the edge **b** is covered with two layers of teflon) and option 3 (light is read from the edge **b** while the edge **a** is covered with two layers of teflon). The results are presented in Fig. 14. Clear correlation between

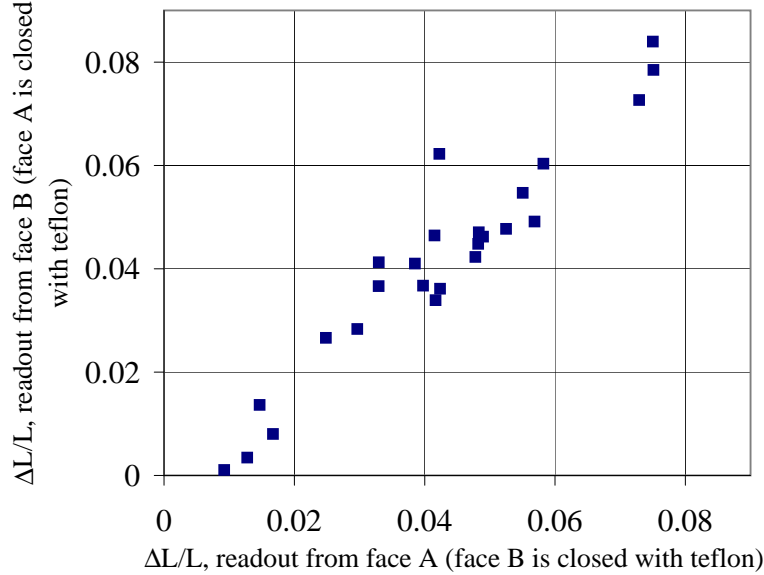


Fig. 14. The correlation between $\Delta L/L$ values measured from the different faces of P-type crystals with options 1 and 3 (see Table 1 for explanation). The absorbed dose is 650 rad.

the measurements performed by two options leads to the conclusion that the uncontrolled variations in the procedure of the detector preparation do not contribute substantially to our measurements.

Fig. 15 shows a comparison of $\Delta L/L$ values for 25 samples of "P" type measured after 650 rad dose irradiation by option 1 (light is read from the edge **a** while the edge **b** is covered with two teflon layers) and option 2 (light is read from the edge **a** while the edge **b** is open). Good correspondence between the results obtained in both options is seen. The light output deterioration with the open rare edge somewhat less than that with covered one.

5 Radiation hardness of the crystals produced from the same ingot

Among the samples of "B" type two pairs of crystals were produced from the same ingot: samples B62 and B67 were cut from one ingot, while both samples B65 and B64 were made from the another one.

The set of "P" crystals contained 8 pairs of such type. In the plot of Fig. 16 the X-axis corresponds to $\Delta L/L$ value for the first crystal from the pair while this value for the second crystal of the same pair is shown along the Y-axis. Presented results were taken for all 10 pairs of crystals after irradiation with the dose of 650-780 rad (a) and dose of 3200 rad (b). As it's seen in the figure the radiation hardness of the crystals produced from the same ingot is the same within the measurement accuracy both for "B" type samples and for

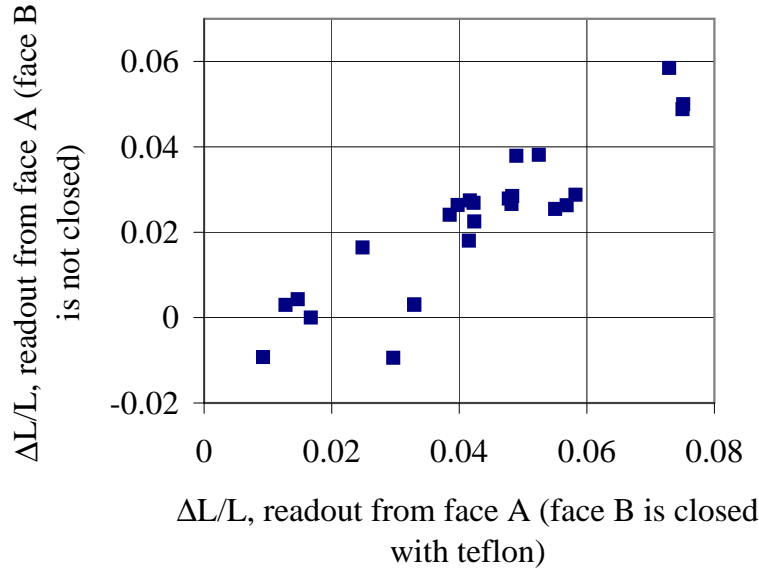


Fig. 15. Correlation between the light output deterioration for crystals of "P" type at the measurement with open and covered rare edge. The absorbed dose is 650 rad.

"P" ones.

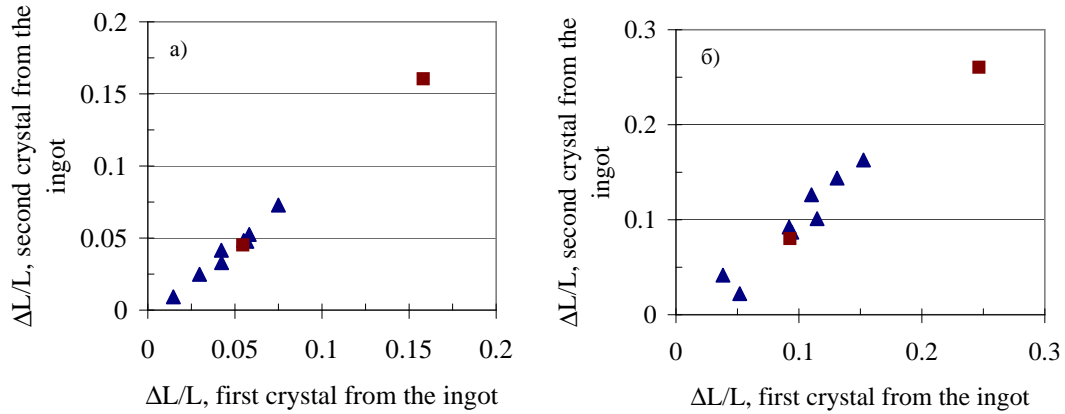


Fig. 16. Correlation between the light output decrease for 10 pairs of samples of both types, produced from the same ingot. The crystals were irradiated with dose 650-780 rad (a) and 3200 rad (b). \blacktriangle – "P" crystals, \blacksquare – "B" samples.

Thus, one has to conclude that the light output deterioration of the irradiated crystals is determined mostly by the properties of grown ingot while the variation of the material properties over ingot volume as well as the uncontrollable changes of the procedure of the crystal processing make much smaller contribution.

The observed correlation provides a possibility for mass control of the radiation hardness of the detectors. It's enough for that to irradiate one sample from each ingot with the desirable dose.

6 Light output self-recovery after irradiation

Some scintillation crystal manifest the natural recovery of the light output damaged due to irradiation. This process was observed for BGO [14], BaF₂ [15], PbWO₄ [16] and for some other materials. Existence of such a recovery for cesium iodide crystals was noted in the works [5, 17].

To study this effect the special measurements with 5 samples of "P" type were performed. The light output and nonuniformity were measured daily during several days before irradiation and after one of 3200 rad. However, it should be remarked that the recovery observation for CsI(Tl) crystals is complicated due to high afterglow that makes the measurements rather inaccurate in the first day after the irradiation.

Fig. 17 presents light output time dependence before and after irradiation for five crystals (P901 - P905). The results for one crystal (P925) which was not irradiated is presented as well for comparison. It's seen that the light output is being recovered with a time constant of a few days up to 20% of the initial radiation damage.

However, the reliable conclusion on the recovery observation can be barely made since the recovery level is not large and we can't exclude that the afterglow can cause some average shift of the signal at the first measurement.

7 Change of the crystal light output nonuniformity after irradiation

Some change of nonuniformity was observed after irradiation with a dose of 3200 rad. For example, Fig. 18 shows the nonuniformity time dependence for several crystals of "P" type. Certain deterioration of light output uniformity is seen for all irradiated crystals after dose of 3200 rad. The nonuniformity of the sample P925 which was not irradiated referred for a comparison. The value of the crystal nonuniformity was defined by the formulae (3).

8 Discussion

Most of the papers devoted to a study of radiation hardness of scintillation crystals consider the optical transparency deterioration as a main reason of light output loss after the irradiation (see, for example, [18, 6]). On the other hand, some authors presented mechanism of the damage of intrinsic scintilla-

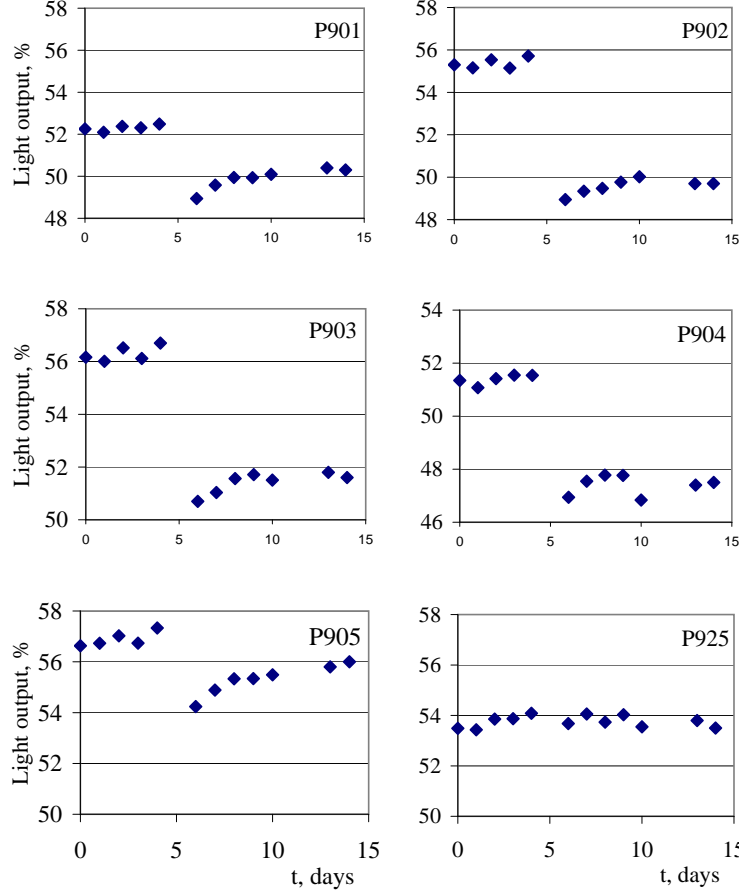


Fig. 17. Time dependence of the crystals light output. Sharp change is connected with the exposition of the crystal with the dose of 3200rad. The results for P925 nonirradiated sample are referred for comparison

tion efficiency of the material due to irradiation [19, 20]. The detail discussion of the physical models of the radiation induced changes of the properties of the scintillation crystals as well as the wide bibliography on this subject can be found in the book [21].

In this work we did not make special studies of the mechanism of the light output degradation. It's worth to remark, however, that during all of the time of this work the dose intensity were measured with only one small CsI(Tl) crystal ($2 \times 2 \times 1cm^3$) which were calibrated time to time. The total dose absorbed by this crystals amounted to 50 krad. Nevertheless, we did not observe considerable decrease of light output of this crystal within few percent of accuracy of measurements . In contrast, the light output loss of the large crystals occur at the much lower absorbed dose that can be explained assuming that the increasing light absorbtion provides the main contribution to the light output degradation.

In general, the inference that the main radiation stimulated effect is the loss of optical transparency of the crystal, looks to be well-grounded, at least for

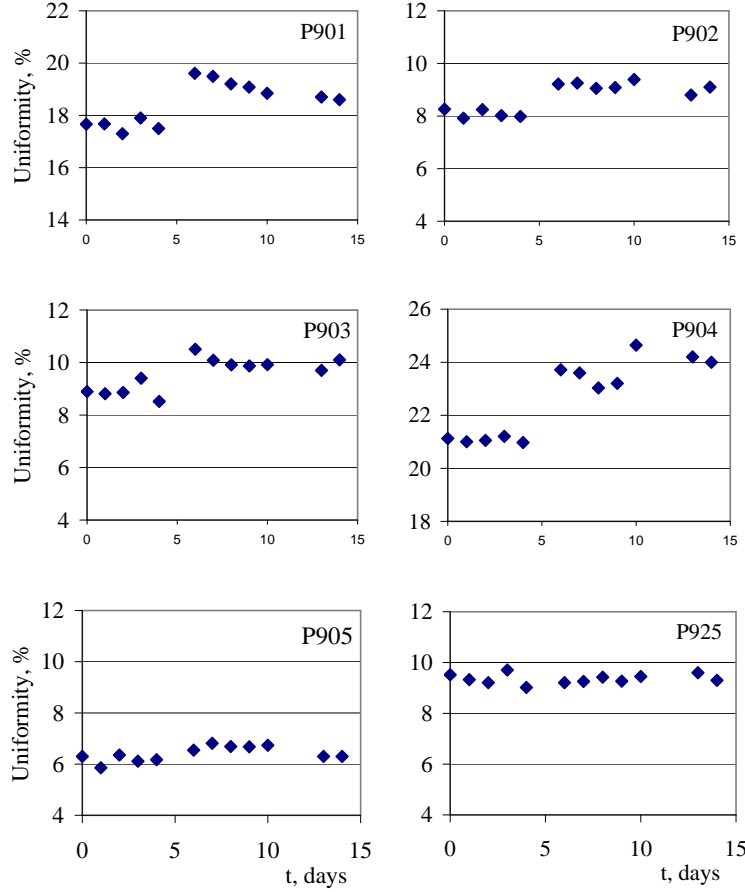


Fig. 18. Time dependence of the nonuniformity of crystals. The step is connected to the irradiation with the dose of 3200rad. Results with non irradiated crystal P925 are referred for comparison.

moderate doses of radiation. Following arguments provide evidence for this:

- the radiation induced absorbtion are really observed in the direct measurements of the optical transparency of crystals [5, 22] and its quantity does not contradict to observed light output decrease for the detectors of real sizes;
- crystals of small sizes demonstrate much lower degradation of light output than the large crystals at the same dose.

It should be noted that besides the loss of the optical transparency, the irradiation can produce both elastic and inelastic centers of photon scattering in the material. This effect can provide the deterioration of the light collection efficiency as well. However, this effect was not carefully studied for CsI crystals.

Let's discuss the results obtained in the sections 4.1 and 4.2. Here, first of all, two features attract an attention: a) large spread of the light output loss values after irradiation for different samples of the same type and b) considerable

average difference in $\Delta L/L$ between samples having the shape of truncated pyramid and parallelepiped.

The conclusion coming from a) is the radiation hardness of the crystals depends strongly from uncontrolled variations in the growing technology from one ingot to the another one. The high correlation between the radiation hardness of the samples produced from the same ingot is the evidence of small variations of the conditions during the growing process. When the radiation hardness is a critical parameter of the detector, the tests for at least one sample cut from each ingot should be performed.

Then we would like to refer some considerations which can explain the effect b). First of all, the light collection conditions for "B" and "P" samples should be considered. The sensitive area of PM tube photocathode, $S_{ph} \approx 16 \text{ cm}^2$, covers completely the output edge of "P" type crystals $S_{out}^P = 4 \text{ cm}^2$, while this coverage is only partial for crystals of type "B", $S_{out}^B = 35 \div 47 \text{ cm}^2$, $S_{ph}/S_{out}^B = 0.35 \div 0.44$. Meanwhile, the average light output for crystals of "B" type is only 15% less than that for "P" crystals. One can suppose that the light collection in "B" crystals involves substantially photons which had multiple reflection at the crystal sides and, possibly, the scattering in the crystal volume. Besides, the shape of the crystal plays substantial role for the light collection. These effects should lead to the increase of the photon mean path before it hits PM tube and, respectively, to the higher sensitivity to the loss of the optical transparency.

The initial values of the light output and the values of $\Delta L/L$ for 19 irradiated crystals of "B" type versus the square, S , of the output crystal face are presented in Fig. 19. Some correlation between light output and S as well as between $\Delta L/L$ and S can be seen in spite of the large spread of data.

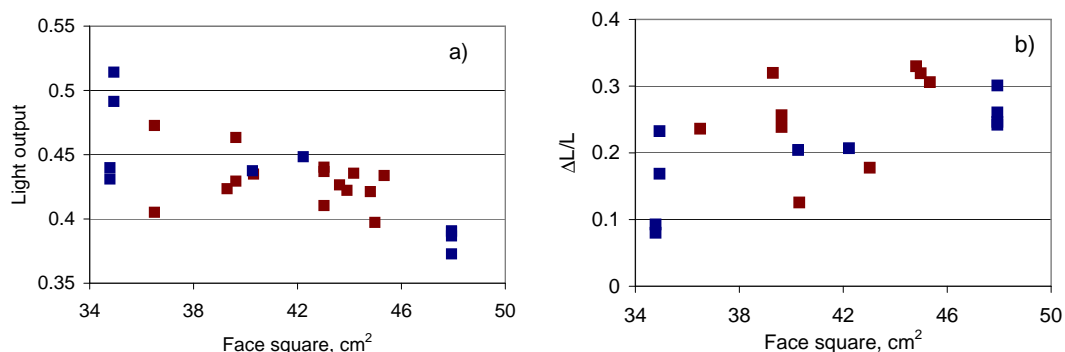


Fig. 19. a) – initial light output of the crystals of "B" type in dependence of the output square; b) – the light output loss for samples of "B" type irradiated with a dose of 3200-3700 rad versus of the square of output face.

9 Conclusion

In conclusion we list the main results of this study:

- In general, all studied crystals have high enough radiation hardness to be used in the detectors for existing B-factories;
- Crystals produced within one technology using the raw material from the same manufacturer demonstrate, nevertheless, large spread of values of radiation stimulated light output loss;
- However, crystals cut from the same ingot have the same level of radiation hardness;
- Large difference in the values of radiation induced light collection efficiency loss for the samples of different geometry was observed. This is an evidence of the substantial dependence of the radiation hardness on the shape of the crystal and light collection conditions.
- There are some samples with high (for alkali halide scintillation crystals) radiation hardness ($\Delta L/L=8\%$ at 3200 rad of absorbed dose). This confirms a principle possibility of the mass production of radiation hard crystals after certain technology upgrade.

Acknowledgements

We are grateful to Prof.R.A.Salimov and Prof.N.K.Kuksanov for the opportunity to use the ELV-6 accelerator. We would like to thank Prof.A.E.Bondar for multiple fruitful and helpful discussions.

A Absorbed dose measurement

The detector of radiation dose in this work based on CsI(Tl) crystal. This detector of $20 \times 20 \times 10 \text{ mm}^3$ size was covered with two layers of the $200 \mu\text{m}$ porous teflon tape. The light signal is read out with a vacuum photodiode (VPD) with massive photocathode. The bias voltage of 40 V is applied as it is shown in Fig. 4. The current through the photodiode is measured.

The choice of the VPD with the solid photocathode is caused by the reason that the measured current can be rather high, up to 10–20 μA . The vacuum photodetectors with semitransparent photocathodes lose the efficiency when the photo current exceeds $\sim 10 \text{ nA}$ due to the disturbance of the electric potential over the cathode surface.

The another option for the scintillation light read out is the usage of the silicon photodiode. But in this case one must take into account the current induced by the interaction of gamma radiation with silicon in addition to the photo current that can decrease the accuracy of the measurement.

The dose rate is determined by the expression:

$$\frac{dD}{dt} = I_D/I_R, \quad (\text{A.1})$$

where I_D — measured photo current, and I_R is the calibration constant, that is equal to the photo current value at the dose rate of 1 rad/sec.

$$I_R = C \cdot m \cdot e \cdot N_e^M \cdot K_\tau, \quad (\text{A.2})$$

where $C=6,24 \times 10^8 \text{ MeV/g}$; m is crystal mass in g; e is an electron charge, N_e^M — normalization constant, the number of electrons passed through photodiode per 1 MeV of the energy absorbed by CsI; K_τ is a correction factor that will be explained later.

Thus, the key task for the described method of the dose measurement is the correct calibration, i.e. a determination of the N_e^M value and, with its help, the value of I_R .

The layout of the DD calibration is presented in Fig. A.1

A photodiode is connected to the input of the charge sensitive preamplifier (CSPA). The output signal comes to the shaping amplifier with the shaping time of 2 μs . The shaped pulse is digitized by the ADC.

At the first stage of the calibration the ADC scale constant was determined, i.e. the number of electrons at the CSPA input pulse that corresponds to

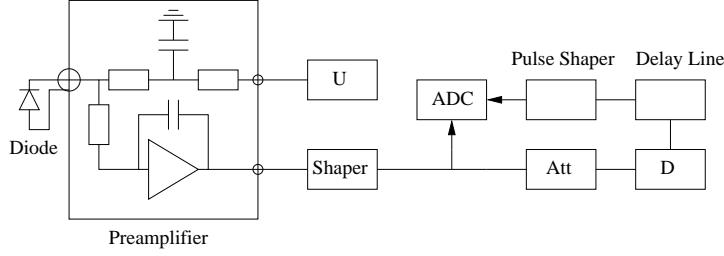


Fig. A.1. The layout of the dose detector calibration. Diode — silicon or vacuum photodiode, Preamplifier — charge sensitive preamplifier, U — voltage source, Att — attenuator, D — discriminator.

one ADC bin. To do that the CSPA input was connected to the silicon PIN photodiode irradiated with γ -quanta of 60 keV energy from ^{241}Am source. The calibration constant was determined as:

$$\kappa = \frac{E_\gamma}{E_i} \cdot \frac{1}{A_{peak}},$$

where A_{peak} is a peak position in the pulse height spectrum, E_i — the average ionization energy for silicon, $E_i = 3.62$ eV.

To measure the signal amplitude corresponding to the 1 MeV energy absorbed in the CsI(Tl) crystal the α -source ^{238}Pu ($E_\alpha = 5.1$ MeV) was used. The direct measurement of this value with γ -source ^{137}Cs (662 keV) or ^{22}Na (511 keV and 1275 keV) was not possible since the noise level was found to be equivalent of 300 keV. To avoid the α -particle absorption in the teflon coverage of the crystal, the small hole of about 1 mm² was made in that. The measured pulse height spectrum is shown in Fig. A.2.

It's known that the scintillation light output for α -particle is lower than that for photons or electrons due to much higher ionization density. The ratio of the signals from ^{238}Pu and total absorption peak of ^{137}Cs was measured separately with the light read out with PM tube. For the crystal used in DD it was found that peak of ^{238}Pu corresponds to 3.71 ± 0.09 MeV of photon energy.

The resulting number of photo electrons per 1 MeV of the energy deposited in the crystal was measured to be $N_e^M = (1180 \pm 30)$ p.e./MeV. It should be noted that for ADC scale calibration the short pulse (about 10 ns) from PIN photodiode was used while the scintillation flash of CsI(Tl) has much longer decay time.

To take this effect into account, the correction factor, K_τ , was implemented to the formulae (A.2). Its value was calculated using the light pulse shape measured in [23] where the experimental shape of this pulse was well approximated by the sum of three exponents with the decay constants of $\tau_1 = 0.7\mu\text{s}$, $\tau_2 = 2.5\mu\text{s}$ and $\tau_3 = 17\mu\text{s}$. As a Laplas representation of the shaper (ORTEC

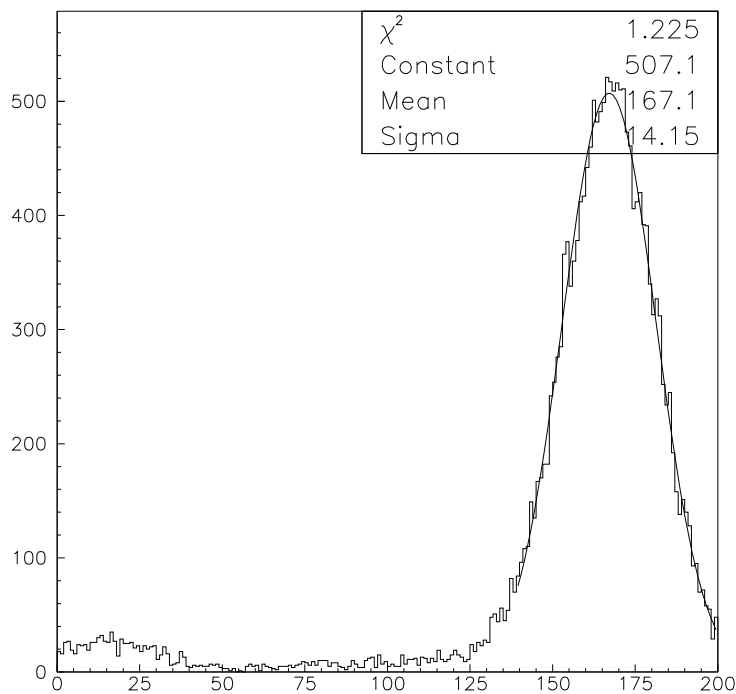


Fig. A.2. ^{238}Pu pulse height spectrum.

370) response function, the following expression was used:

$$K_L(p) = \frac{p}{\tau_s^2(p + 1/\tau_s)^3},$$

where τ_s is the shaping time. This formula implied the single differentiation and double integration provides good approximation of the output pulse shape that corresponds to the input step pulse. The measured value of the correction factor was $K_\tau = 1.4$.

As a result of the described calibration procedure the value of $I_R = 0.3\mu\text{A}\cdot\text{s}/\text{rad}$ was obtained. This procedure was repeated several times with the interval of several months giving the close results of I_R .

We estimate the relative error of the absorption dose measurement with the described method by about 10%. The main contributions to the inaccuracy are connected with the inexact description of the slow components of scintillator decay time as well as with precision of the measurement of α/γ ratio.

REFERENCES

1. R.S.Kessler *et al.*, Nucl. Inst. &Meth., **A368** (1996) 653.
2. K.Miyabayashi (For the Belle Electromagnetic Calorimeter Group) Nucl. Inst. &Meth., **A494** (2002) 298.
3. M.Kobayashi and S.Sakuragi, Nucl. Inst. &Meth., **A254** (1987) 275.
4. D. Renker, Proc. of 4th Topical Seminar on Perspectives for Experimental Apparatus for High-energy Physics and Astrophysics, San Miniato, Italy, 1990, p.350-356.
5. K.Kazui, *et al.*, Nucl. Inst. &Meth., **A394** (1997) 46.
6. M.A.H.Chowdhury, *et al.*, Nucl. Inst. &Meth., **A432** (1999) 147.
7. M.Yamauchi, Nucl. Phys. B (Proc.Suppl.) **111** (2002) 96.
8. D.Hitlin, **A494** Nucl. Inst. &Meth., (2002) 29.
9. A.Abashian, *et al.*, (Belle collaboration), Nucl. Inst. &Meth., **A479** (2002) 117.
10. S.B.Oreshkin, Magister thesis (in Russian), Novosibirsk State University, Novosibirsk, 1996.
11. Belle collaboration, Progress report, KEK Progress Report 97-1, April 1997.
12. B.Shwartz, Nucl. Inst. &Meth., **A453** (2000) 205.
13. Yu.I.Golubenko, *et al.*, Preprint BINP 97-7 (in Russian), Novosibirsk 1997.
14. G.J.Bobbink, *et al.*, Nucl. Inst. &Meth., **A227** (1984) 470.
15. R.Y.Zhu, Nucl. Inst. &Meth., **A340** (1994) 442.
16. R.Y.Zhu, *et al.*, Nucl. Inst. &Meth., **A376** (1996) 319.
17. R.Y.Zhu, *et al.*, Proc. 6th Int. Conf. on Calorimetry in High Energy Physics, Frascati Physics Series, 1996, p.577.
18. R.Y.Zhu, Nucl. Inst. &Meth., **A413** (1998) 297.
19. M.E.Globus and B.V.Grinyov, Functional materials, **3**, No.2 (1996) 231.
20. A.V.Gektin, Proc. of The 5th Int. Conf. on Inorganic Scintillators and their Applications, Moscow, 1999, p.79.
21. M.E.Globus and B.V.Grinyov, Inorganic scintillators (in Russian), Akta, Kharkov, 2000.
22. L.N.Shpilinskaya, *et al.*, Proc. of The 5th Int. Conf. on Inorganic Scintillators and their Applications, Moscow, 1999, p.79.
23. A.Yu.Garmash, Magister thesis (in Russian), Novosibirsk State University, Novosibirsk, 1998.